

## Synthesis and Characterization of the Layered $K_2NiF_4$ Type $(C_nH_{2n+1}NH_3)_2PbCl_4$ System

Soo Jung Lee, Gwe Ya Kim, Eung-Ju Oh,<sup>†</sup> Keu Hong Kim, and Chul Hyun Yo<sup>\*</sup>

Department of Chemistry, Yonsei University, Seoul 120-749, Korea

<sup>†</sup>Department of Chemistry, Myongji University, Yongin 449-728, Korea

Received June 17, 1999

Layered  $K_2NiF_4$ -type  $(C_nH_{2n+1}NH_3)_2PbCl_4$  ( $n=6, 8$  and  $10$ ) system, or alkylammonium tetrachloroplumbate compound, has been synthesized from  $PbCl_2$  and  $C_nH_{2n+1}NH_3Cl$  solutions under argon ambient pressure for 12hrs at  $90^\circ C$ . The crystal structure of the compound has been analyzed using X-ray powder diffraction in the range of  $5^\circ < 2\theta \leq 55^\circ$ , and all samples assigned to an orthorhombic system. Local distances of the Pb-Cl bond have been determined by Pb L<sub>III</sub>-edge extended X-ray absorption fine structure (EXAFS) spectroscopy. The vibration modes of alkylammonium chains and the absorption peaks of an exciton have been examined by FT-IR and UV-Vis. reflectance spectra, respectively. The phase transition temperatures of the compounds have been studied by using DSC. According to the thermal analysis, two phase transition temperatures have been observed in the compositions of  $n=8$  and  $10$ .

### Introduction

During the last decade,  $K_2NiF_4$ -type organic-inorganic layered compounds were actively studied because of their two dimensional structure.<sup>1-2</sup> The layered compounds with a general formula  $(C_nH_{2n+1}NH_3)_2MX_4$  where  $M=Cd, Pb, Mn, Cu, Fe, Pd$  and  $X=Cl, Br, I$  have a bilayer of alkylammonium chains, which acts as an energy barrier that intercepts the interaction between the inorganic layers.<sup>3</sup>  $MCl_4^{2-}$  inorganic layers are built up on corner-shared halogen octahedra with an  $M^{2+}$  ion at the center. Organic layers are built up on the  $NH_3^+$  headed alkyl chains, which are placed in a cavity of the octahedron axial chlorides. Alkyl tails are extended toward both sides of an inorganic layers.

A portion of the compound with the general formula,  $(C_nH_{2n+1}NH_3)_2MX_4$ , is shown in Figure 1. The organic layers control the flexibility of the compound with changes in the alkylammonium chain length. The inorganic layers control the thermal stability, magnetic property, and electrical con-

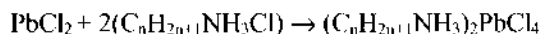
ductivity of the compound. The structures of  $K_2NiF_4$ -type layered compounds are stabilized by a van der Waal's interaction between organic layers, a Coulombic force between the positive  $C_nH_{2n+1}NH_3^+$  and negative  $SnCl_4^{2-}$  charges, and a hydrogen bond between the hydrogen atom of alkylammonium polar head and the halogen atom in the inorganic layer.<sup>4</sup>

The exciton binding energy of the two-dimensional compound has been observed to be four times that of the three-dimensional compound, which is due to a dielectric confinement effect.<sup>5</sup> The  $K_2NiF_4$ -type compounds show two-dimensional behavior and are applicable in nonlinear optical, photoluminescent, and electroluminescent devices.<sup>6</sup> The phase transition is due mainly to two reasons: One is that an order-disorder transition of rigid alkyl ammonium chains includes a partial "melting". The other is conformational changes in the chains, defined as the rapid diffusion of one or more gauche bonds up and down the chain.<sup>7</sup>

In this paper, we present a low temperature (below  $100^\circ C$ ) aqueous solution method for preparing organic-inorganic two dimensional compounds. To determine the coupling state between the organic and inorganic layers, UV, FT-IR spectroscopies were used. XRD and EXAFS spectroscopies were used to determine the crystallographic structure. Thermal stability was investigated by DSC.

### Experimental Section

The compounds of the  $(C_nH_{2n+1}NH_3)_2PbCl_4$  system were synthesized by mixing the *n*-alkylammonium chloride derived from the corresponding amine and the lead chloride with stoichiometric ratio in hydrochloric acid solutions.



The mixtures were reacted at  $90^\circ C$  for 12 hours under

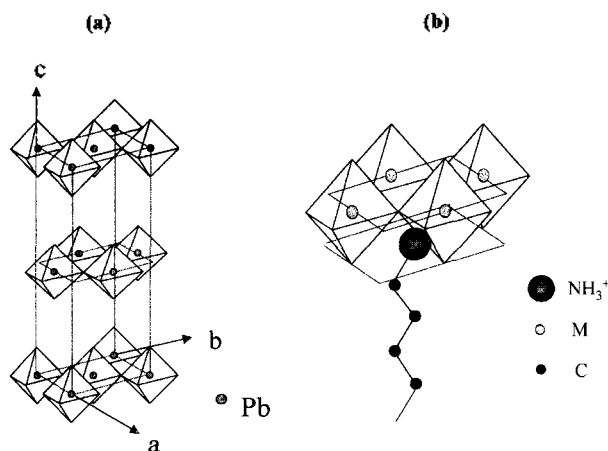


Figure 1. (a) Schematic unit-cell structure of  $(C_nH_{2n+1}NH_3)_2PbCl_4$  and (b) a part of  $(C_nH_{2n+1}NH_3)_2PbCl_4$ .

flowing Ar gas to prevent the oxidation. The crystalline precipitates were produced by slow cooling from 90 °C to -10 °C. The structure of the samples was analyzed by Philips pw 1710 X-ray diffractometer with Ni-filtered Cu K $\alpha$  radiation in a range of  $5^\circ \leq 2\theta \leq 55^\circ$ . Extended X-ray absorption fine structure (EXAFS) spectra of the Pb L<sub>II</sub>-edge were recorded with the ring current of 100-120 mA at the BL3C1 of PLS (Pohang light source).

Infrared spectroscopic measurements were carried out to obtain data on the alkylammonium chains from 1300 cm<sup>-1</sup> to 3300 cm<sup>-1</sup> at room temperature. The mixed powder of the sample and KBr is used for the IR spectra measurements, recorded with a Bruker IFS66 spectrometer. The reflectance spectra were measured using a highly-reflecting mirror-mounted Shimadzu UV-3100 in a range of 200 nm to 800 nm.

The phase transition temperature and thermal stability of the layered (C<sub>n</sub>H<sub>2n+1</sub>NH<sub>3</sub>)<sub>2</sub>PbCl<sub>4</sub> compounds were determined by a Perkin Elmer DSC7 for the temperature ranges of -50 °C to 50 °C and 50 °C to 100 °C.

## Results and Discussion

**X-ray diffraction spectroscopic analysis.** Structural information was investigated by the powder XRD method. The compounds of n=1, 2, 3, and 4 in the (C<sub>n</sub>H<sub>2n+1</sub>NH<sub>3</sub>)<sub>2</sub>PbCl<sub>4</sub> did not exhibit good solid solutions. Therefore, the discussion covers only the cases n=6, 8, and 10 in (C<sub>n</sub>H<sub>2n+1</sub>NH<sub>3</sub>)<sub>2</sub>PbCl<sub>4</sub>. The peaks shift of (00l) to lower 2 $\theta$  with increasing n value corresponds with increases in the c parameter. Well-defined (00l) and other small (hkl) reflections are clearly observed in the cases of n=6, 8, 10 in (C<sub>n</sub>H<sub>2n+1</sub>NH<sub>3</sub>)<sub>2</sub>PbCl<sub>4</sub>.

The XRD patterns and interlayer distances between inorganic layers are proportional to the n values, as shown in Figure 2. The organic chains are arranged to the great extent

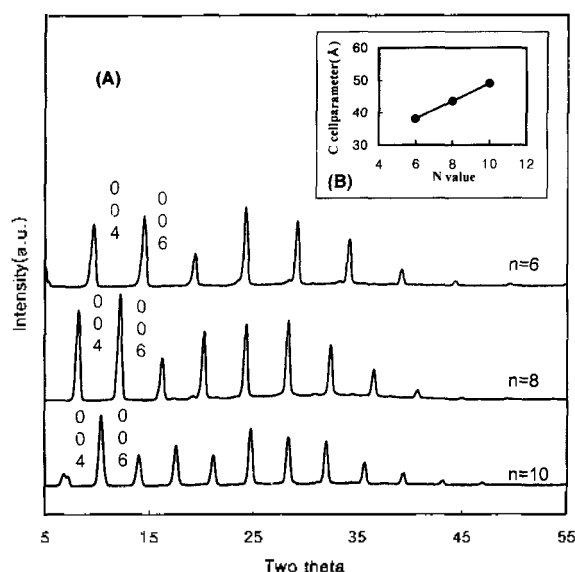


**Figure 2.** (A) X-ray diffraction patterns for the (C<sub>n</sub>H<sub>2n+1</sub>NH<sub>3</sub>)<sub>2</sub>PbCl<sub>4</sub> and (B) c parameter changes with n value in the (C<sub>n</sub>H<sub>2n+1</sub>NH<sub>3</sub>)<sub>2</sub>PbCl<sub>4</sub>.

**Table 1.** Lattice parameters, lattice volume, and crystal system for the (C<sub>n</sub>H<sub>2n+1</sub>NH<sub>3</sub>)<sub>2</sub>PbCl<sub>4</sub> system

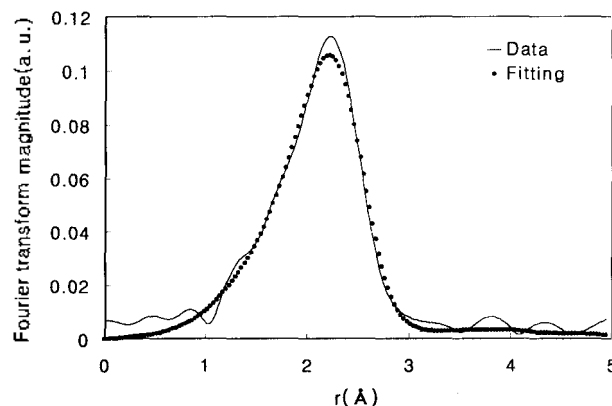
Compound (n value)	Lattice parameter (Å)			V (Å <sup>3</sup> )	Crystal system
	a	b	c		
6	7.78(6)	7.93(3)	38.1(4)	2356	orthorhombic
8	7.82(9)	7.96(3)	43.5(5)	2715	orthorhombic
10	7.86(2)	7.98(9)	49.0(9)	3083	orthorhombic

in the same direction. The lattice parameters, lattice volumes, and crystal systems are listed in Table 1. The crystallographic structure of all compounds is assigned to an orthorhombic system.

**EXAFS spectroscopy.** To determine the local structure around Pb, EXAFS analysis was performed. The EXAFS data were analyzed using a nonlinear fitting method and computer code FEFF6 (University of Washington). The best-fit of Fourier transformations spectra are shown in Figure 3 for the case of n=6 in (C<sub>n</sub>H<sub>2n+1</sub>NH<sub>3</sub>)<sub>2</sub>PbCl<sub>4</sub>, the other fitted spectra similar to the hexyl ammonium tetrachloroplumbate. The bond length of Pb-Cl shows different values along the x, y, z axes. Structural parameters of the (C<sub>n</sub>H<sub>2n+1</sub>NH<sub>3</sub>)<sub>2</sub>PbCl<sub>4</sub> system obtained from Pb L<sub>II</sub>-edge EXAFS spectra are listed in Table 2.

In (C<sub>n</sub>H<sub>2n+1</sub>NH<sub>3</sub>)<sub>2</sub>PbCl<sub>4</sub>, the stereochemical activity of the Pb(II) nonbonding electrons is apparent from the distorted octahedral coordination of chlorines with variable Pb-Cl bonds in the a-b plane of the perovskite layers. Typically, the stereoactivity of the lone pair electron is significant for divalent group B cations.<sup>4,8</sup> From the bondlength and Debye-Waller factor, we can confirm that very tight bounded and distorted inorganic layer is present and will lead to low carrier mobility. This is also confirmed by conductivity measurement, which shows poor conductivity (<10<sup>-10</sup> S/cm) for a pellet sample.

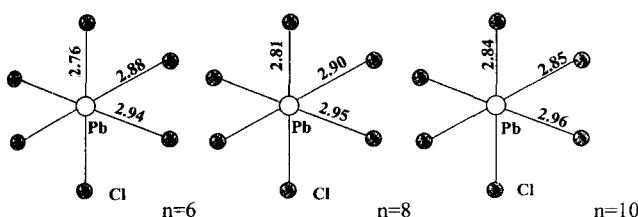
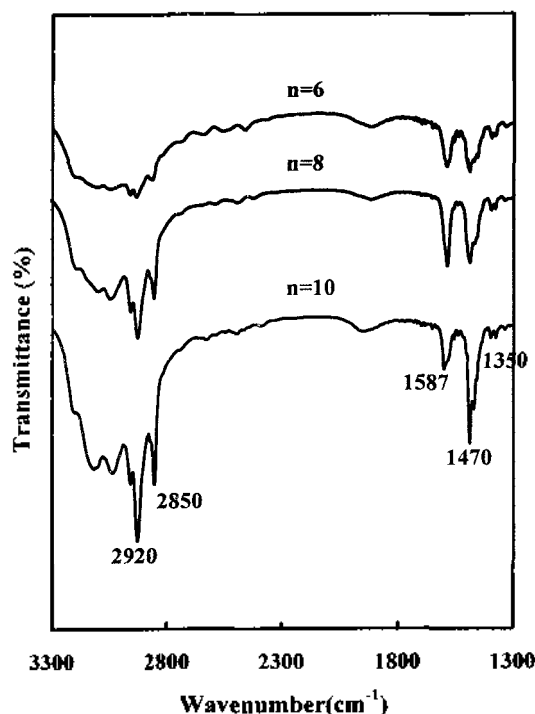
**FT-IR spectroscopy.** Figure 5 shows FT-IR spectra of the (C<sub>n</sub>H<sub>2n+1</sub>NH<sub>3</sub>)<sub>2</sub>PbCl<sub>4</sub> system at room temperature. In the infrared spectrum between 1300 cm<sup>-1</sup> and 3300 cm<sup>-1</sup>, a number of modes correspond to the vibrations, which involve the entire chain and give rise to progressive bands. Their wave



**Figure 3.** Experimental (solid line) and calculated (dot) Fourier Transform magnitude of the Pb L<sub>II</sub>-edge EXAFS spectra for the compounds of n=6 in the (C<sub>n</sub>H<sub>2n+1</sub>NH<sub>3</sub>)<sub>2</sub>PbCl<sub>4</sub> system.

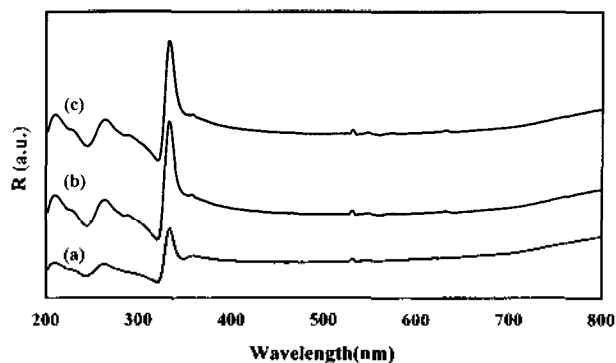
**Table 2.** Structural parameters from Pb L<sub>III</sub>-edge EXAFS spectra for the  $(C_nH_{2n+1}NH_3)_2PbCl_4$  system

n	Path	N	Amp.	$E_0$ (eV)	r (EXAFS) (Å)	Debye-Waller factor
6	Pb-Cl(1)	2	0.7	0.03	2.88(3)	0.020
	Pb-Cl(2)	2		-14.7	2.76(0)	
	Pb-Cl(3)	2		-0.35	2.93(7)	
8	Pb-Cl(1)	2	1.1	0.08	2.80(7)	0.020
	Pb-Cl(2)	2		0.57	2.95(4)	
	Pb-Cl(3)	2		-10.6	2.90(4)	
10	Pb-Cl(1)	2	0.7	-0.04	2.83(8)	0.007
	Pb-Cl(2)	2		-4.97	2.85(1)	
	Pb-Cl(3)	2		4.08	2.89(8)	

**Figure 4.** The distances of the Pb-Cl in the  $(C_nH_{2n+1}NH_3)_2PbCl_4$  system.**Figure 5.** FT-IR spectrum of the  $(C_nH_{2n+1}NH_3)_2PbCl_4$  system.

number and intensity depend on both the length and the configuration of the chain.

The asymmetric and symmetric stretching modes of  $CH_2$  appeared at  $2900\text{ cm}^{-1}$  and  $2850\text{ cm}^{-1}$ , respectively. The bending mode of  $CH_2$  is shown at  $1470\text{ cm}^{-1}$  and the  $CH_2$  wagging modes are presented in a range of  $1350\text{ cm}^{-1}$  to  $1300\text{ cm}^{-1}$ .<sup>9</sup> The wavenumbers are very similar to the wavenum-

**Figure 6.** Reflection spectra for the composition of (a)  $n=6$ , (b)  $n=8$  and (c)  $n=10$  in the  $(C_nH_{2n+1}NH_3)_2PbCl_4$ .

bers of their alkyl ammonium monomer's vibration mode ( $2926\text{ cm}^{-1}$ ,  $2855\text{ cm}^{-1}$ ,  $1468\text{ cm}^{-1}$ , and  $1379\text{ cm}^{-1}$  respectively). It means that the organic layer is not strongly coupled to the inorganic layer even for small  $n$  values.

**Reflectance spectroscopy.** The reflectance absorption spectra for the compounds of  $n=6$ , 8, and 10 in the  $(C_nH_{2n+1}NH_3)_2PbCl_4$  system at room temperature show an exciton band (Figure 6) located at  $332\text{ nm}$ .<sup>10</sup> This shows that the transition occurred in the inorganic layer, which is confirmed because the alkylamine is transparent in the visible region. The similar exciton band positions also show that the inorganic layers are weakly coupled with organic layers.

Imagine an ultrathin quantum well with a dielectric constant of  $\epsilon_1$  sandwiched with barrier layers of  $\epsilon_2$ , when smaller  $\epsilon_2$  are presented ( $\epsilon_2=2.44$  in  $(C_{10}H_{21}NH_3)_2PbCl_4$  and  $\epsilon_2=3.32$  in  $(C_6H_5C_2H_4NH_3)_2PbCl_4$ ), the exciton binding energy is decreased ( $320\text{ meV}$  in  $(C_{10}H_{21}NH_3)_2PbCl_4$  and  $220\text{ meV}$  in  $(C_6H_5C_2H_4NH_3)_2PbCl_4$ ).<sup>11</sup> The larger difference in the dielectric constants between the organic and inorganic layers will lead to high-performance quantum-well structures. In these compounds, the dielectric constant of the organic barrier layer is much smaller than the inorganic perovskite layer. It shows the dielectric confinement effect and four times the exciton binding energy compared with their 3D structure.<sup>12</sup> Usually, this type of material can be applied to semiconductor devices as a quantum-well structure. The valence bands are largely represented by the in-plane 3D orbitals of the Cl atoms, which combine out-of phase (*i.e.* antibonding) with the Pb 6s orbitals. The conduction bands are primarily given by the Pb 6p orbitals.<sup>13</sup> The absorption peak might be assigned to the electron transition from  $Pb(6s)+Cl(3p)$  to  $Pb(6p)$ .<sup>11</sup>

**Thermal analysis.** According to DSC measurements, two phase transitions have been recorded for the compounds of  $n=8$  and 10, as shown in Figure 7. They define the domains of three phases named I, II, III. The transition temperature, enthalpy change, and entropy change of the  $(C_8H_{17}NH_3)_2PbCl_4$  and  $(C_{10}H_{21}NH_3)_2PbCl_4$  compounds are listed in Table 3. Entropy change calculated from the relation  $\Delta S = \Delta H/T$ . The main transition in these compounds should be a partially-chain melting transition.<sup>14</sup> The other transition is expected with dynamic two-fold rotational disordering of the chains.<sup>15</sup> The main transition temperature increases with longer alkyl

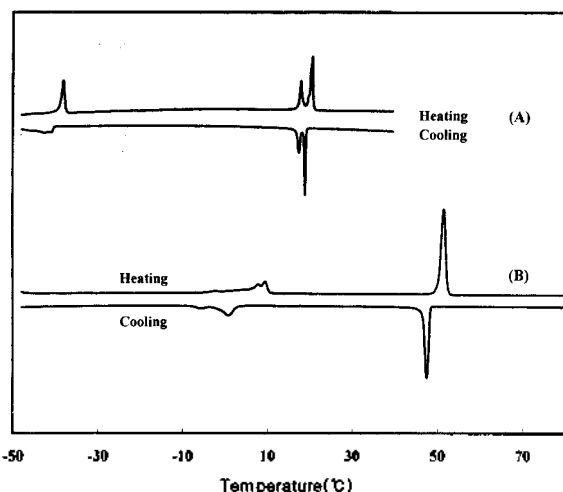


**Figure 7.** DSC results concerning the phase transition (A)  $n=8$  and (B)  $n=10$  in the  $(C_nH_{2n+1}NH_3)_2PbCl_4$ .

**Table 3.** Transition temperature, enthalpies, and entropies of the  $(C_8H_{17}NH_3)_2PbCl_4$  and  $(C_{10}H_{21}NH_3)_2PbCl_4$  compounds obtained by the DSC

n	Transition		T(K)	$\Delta H$ (kJ/mol)	$\Delta S$ (J/Kmol)
8	I $\rightarrow$ II	heating	235.1	9.490	40.40
	II $\rightarrow$ III	heating	293.7	18.17	629.9
10	I $\rightarrow$ II	heating	269.6	0.300	1.100
	II $\rightarrow$ III	heating	281.8	8.440	29.90

chains in the compounds. It is obvious that larger van der Waal's interactions, which hinder the phase transition occurs.

### Conclusion

Two dimensional organic-inorganic  $(C_nH_{2n+1}NH_3)_2PbCl_4$  compounds were synthesized by low temperature aqueous solution technique. All samples were assigned to the orthorhombic system. They showed different bondlength of Pb-Cl along x, y, z axes. The UV, FT-IR, and XRD patterns showed

two dimensional characteristics even though n was not abnormally large ( $n \geq 6$  in  $(C_nH_{2n+1}NH_3)_2PbCl_4$ ). The two phase transitions have been observed for  $n=8$  and 10 in  $(C_nH_{2n+1}NH_3)_2PbCl_4$ .

**Acknowledgment.** The present study was supported by the Basic Science Research Institute Program, Ministry of Education of Korea, 1997, Project No. BSRI-97-3424. We thank Dr. Jay Min Lee and Pohang Light Source for their help on the EXAFS measurement.

### References

1. Calabrese, J.; Jones, N. L.; Harlow, R. L.; Herron, N.; Thorn, D. L.; Wang, Y. *J. Am. Chem. Soc.* **1991**, *113*, 2328.
2. Kondo, T.; Iwamoto, S.; Hayase, S.; Tanaka, K.; Ishi, J.; Mizuno, M.; Ema, K.; Ito, R. *Solid State Comm.* **1998**, *105*(8), 503.
3. Koutselas, I. B.; Ducasse, L.; Papavassiliou, G. *C.J. Phys.: Condens. Matter* **1996**, *8*, 1217.
4. Mitzi, D. B. *Chem. Mater.* **1996**, *8*, 791.
5. Muljarov, E. A.; Tikhodeev, S. G.; Gippius, N. A. *Physcal Review B* **1995**, *51*(20), 14370.
6. Era, M.; Morimoto, S.; Tsutsui, T.; Saito, S. *Appl. Phys. Lett.* **1994**, *65*(6), 676.
7. Zerbi, G.; Mortz, K.; Bigotto, A.; Dirlikov, S. *J. Chem. Phys.* **1981**, *75*(7), 3175.
8. Mitzi, D. B.; Fellid, C. A.; Harrison, W. T. A.; Guloy, A. M. *Nature* **1994**, *369*, 467.
9. Guo, N.; Zeng, G.; Xi, S. *J. Phys. Chem. Solids* **1992**, *53*(3), 437.
10. Papavassiliou, G. C.; Patsis, A. P.; Lagouvardos, D. J.; Koutselas, I. B. *Synthetic Metals* **1993**, *55-57*, 3889.
11. Ishihara, T. *J. Luminescence* **1994**, *60&61*, 269.
12. Kitazawa, N. *Jpn. J. Appl. Phys.* **1996**, *35*, 6202.
13. Papavassiliou, G. C.; Koutselas, I. B.; Terzis, A.; Whangbo, M. H. *Solid State Comm.* **1994**, *91*(9), 695.
14. Yin, R. Z.; Yo, C. H. *Bull. Korean Chem. Soc.* **1998**, *19*(9), 947.
15. Needham, G. F.; Willet, R. D.; Franzen, H. F. *J. Phys. Chem.* **1984**, *88*, 674.